Available online at www.sciencedirect.com
SCIENCE DIRECT®

Journal of the European Ceramic Society 23 (2003) 2135–2142
www.elsevier.com/locate/jeurceramsoc

Structural study of $LaNi_xFe_{1-x}O_3$ prepared from precursor salts

E. Bontempi[a], C. Garzella[b], S. Valetti[a], L.E. Depero[a,*]

[a]*Structural Chemistry Laboratory, Dipartimento di Ingegneria Meccanica and INSTM, Università di Brescia, via Branze 38, 25123 Brescia, Italy*
[b]*Dipartimento di Chimica e Fisica per l'Ingegneria e i Materiali and I.N.F.M., Università di Brescia, via Valotti 9, 25123 Brescia, Italy*

Received 5 September 2002; received in revised form 8 December 2002; accepted 15 December 2002

Dedicated to the memory of Professor E. Tempesti

Abstract

$LaNiO_3$, $LaFeO_3$ and their solid solution $LaNi_{0.3}Fe_{0.7}O_3$ have been prepared using acetate and citrate salts as precursors. The decomposition of organic substances were obtained by calcination in mild conditions. A detailed discussion of the structural and microstructural changes of these materials due to thermal treatments is proposed by means of X-ray diffraction, microraman spectroscopy, and scanning electron microscopy studies. Moreover, the local distortion of the perovskite structure determining the second order transition in these perovskites has been evidenced by microraman spectroscopy. Indeed, this technique has been shown to be powerful to characterize the local coordination of the metals, that is possibly a critical parameter in their chemical activity.
© 2003 Elsevier Science Ltd. All rights reserved.

Keywords: Calcination; La(Ni,Fe)O_3; Perovskites; Raman spectroscopy; X-ray methods

1. Introduction

Perovskite-type oxides (ABO_3, where A is an alkali, alkaline earth, or lanthanide metal and B is a transition metal) are widely studied for their intrinsic properties[1] and their applications in electrochemistry,[2] superconductivity[3] and catalysis.[4] Their composition can be varied in a wide range by partial substitution of cations in A and/or B sites yielding compounds of the general formula $(A_xA'_{1-x})(B_yB'_{1-y})O_3$ with different physical and chemical properties. The cation substitution may induce distortions in the perovskite structure[5,6] and a great stability up to high temperatures.

It was also reported that substituted $LaMO_3$ materials (where M is a transition metal) are interesting for the combustion of hydrocarbons,[7] and in particular for methane.[8] In particular, studies performed on $LaNiO_3$[9] evidenced that nickel into this type of structure stabilizes the active metal at high temperature and it limits the sintering and the coke formation. Moreover, the combination of nickel with a second element of the VIII group into a lanthanum phase (La(Ni,M)O_3) generally forms perovskite structures. Also in this case the strong interactions between nickel and the perovskite structure limits crystallites growth and carbon deposition.[10]

Provendier et al.[11] obtained $LaNiO_3$, $LaFeO_3$ and $LaNi_xFe_{1-x}O_3$ from aqueous solutions of the precursors with addition of oxalic acid and precipitation of the oxides, while Delmon et al. have proposed 30 years before a citrate route.[12] More recently, Kienemann and co-workers[13,14] have proposed a sol-gel method which allows the synthesis of $LaNi_xFe_{1-x}O_3$ perovskite single phase by using the propionic acid as the solvent. The critical point of this method is the decomposition of nitrate anions with violent NO_2 production which is especially observed in large scale preparations during the evaporation of the solvent. At this regards, this method is even more dangerous than the original route based on citrate because of the presence of propionic acid instead of water.

For the first time, in this paper the evolution of the structure, microstructure, and morphology due to different temperature treatments of $LaNiO_3$, $LaFeO_3$, and $LaNi_{0.3}Fe_{0.7}O_3$ powders is reported. The samples preparation is based on a variation of the Delmon method.

We have modified the citrate route by:

(a) utilizing acetates instead of nitrates as starting salts and

* Corresponding author.
E-mail address: depero@ing.unibs.it (L.E. Depero).

0955-2219/03/$ - see front matter © 2003 Elsevier Science Ltd. All rights reserved.
doi:10.1016/S0955-2219(03)00026-8

(b) decomposing the organic substances in mild conditions by typical temperatures up to 400° C.

The $LaNi_{0.3}Fe_{0.7}O_3$ composition was chosen because Provendier et al.[15] have demonstrated that within the series $LaNi_xFe_{1-x}O_3$ the perovskite with $x=0.3$ presented the best catalytic activity. Moreover, similar sample was also analysed by Rapagnà et al. to develop a catalyst for hydrogen production from biomass gasification.[16] It results that the $LaNi_{0.3}Fe_{0.7}O_3$ shows the best activity at the temperature of 800 °C.

2. Experimental section

2.1. Preparation method

The major advantages of this preparation procedure, referring to the method based on nitrates mainly used as precursors,[13,14] implies the absence of propionic acid as the solvent, that may cause safety and environmental problems.

The preparation of $LaNi_{0.3}Fe_{0.7}O_3$ was carried out starting from three different precursor solutions. Lanthanum(III)acetate hydrate 5.3 g, nickel(II)acetatetetrahydrate 1.064 g and iron(III)citrate 2.936 g were separately dissolved in water. The three solution were then mixed together and appropriate amount of citric acid (1 equivalent of citric acid per equivalent of cation) and ammonia were added. NH_3 allows all the components to be in the solution. The solution was then concentrated in a rotavapor by rising the temperature up to 90 °C at 100 mbar until the formation of a meringue-type spongy solid. The sample was dried in a vacuum oven starting from 70 to 180 °C with a linear increase of temperature in 5 days (15 °C/12 h) and then heated at 400 °C (6 °C/h, 2 h at 400 °C) in order to obtain the complete decomposition of the organic phases. Finally, different samples were thermally treated in air at 600, 700, 800, 900 and 1000 °C (15 °C/h, 2 h at the final temperature). $LaNiO_3$ and $LaFeO_3$ were prepared using the same method starting from the respectively metallic precursors.

2.2. Characterization techniques

All the X-ray diffraction experiments were performed by a Philips MPD 1830 automated powder diffractometer with graphite-monochromated CuK_α radiation in the Bragg-Brentano parafocusing geometry. The spectra were collected between 10 and 80° (2θ range), with an angular step of 0.02°. For the phase identification the JC-PDF database[17] and the EVA search/match software[18] were used. The XRD pattern were analysed by means of the Topas P software.[19]

Microraman spectra were collected by a Dilor Labram spectrograph. The exciting source was a HeNe laser (632.8 nm) with a power of less than 10 mW at the sample. The microscope was couple confocally to the spectrograph. A 50× objective with a numerical aperture NA = 0.9 and a confocal hole opened at 300 μm were used. Suppression of the exciting line was obtained with a holographic notch filter. The spectra were measured at room temperature.

SEM observations have been carried out with a Cambridge S260 microscope equipped by EDX system. The micrographs have been recorded at 20 kV and the samples have been sputtered by gold.

3. Results and discussion

XRD patterns of $LaFeO_3$, $LaNi_{0.3}Fe_{0.7}O_3$, and $LaNiO_3$ were collected after calcination treatments performed at 600, 700, 800, 900 and 1000 °C. All the observed XRD patterns presented sharp reflections, showing that the materials are well crystallized after all the temperature treatments. It is important to note that even $LaNi_{0.3}Fe_{0.7}O_3$ samples appeared to be monophasic after the thermal treatments. This is evidence that solid solutions of Ni and Fe in the perovskite structure can be obtained by the preparation method described above. Indeed, the main effect of the Ni in the $LaFeO_3$ structure seems to be the inhibition of the crystallites growth (see the discussion below).

For treatments at temperatures lower than 800 °C, both $LaFeO_3$ and $LaNi_{0.3}Fe_{0.7}O_3$ materials the XRD patterns were indexed by a cubic perovskite structure, while for high temperature treatments (900 and 1000 °C) small reflections characteristic of the orthorhombic phase were detected. The patterns of the cubic and the orthorhombic phases obtained for the $LaFeO_3$ sample at 600 and 1000 °C are shown in Fig. 1. Similar patterns are obtained for $LaNi_{0.3}Fe_{0.7}O_3$ samples, the only difference being a shift of the reflections due to slighter different cell parameters. Therefore we concluded that the stable phase for the $LaFe_{1-x}Ni_xO_3$ with $x=0.3$ is the orthorhombic perovskite. This result is in agreement with the literature,[20] where the structure of $LaFe_{1-x}Ni_xO_3$ was found to be orthorhombic for $x<0.5$ and rhombohedral for higher x values, even if it has recently been reported a rhombohedral structure for $LaNi_{0.3}Fe_{0.7}O_3$.[21] These contradictory results may be due to the influence of the oxygen stoichiometry on the phase formation. The cubic phase detected at low temperatures can be ascribed to some disorder in the perovskite structure. Indeed, many examples can be found in the literature in which the high symmetry of the XRD patterns is determined by disorder effects.[22,23]

In Fig. 2 the XRD patterns obtained for $LaNiO_3$ treated at different temperatures are reported. For clarity, the expansion of the 31–35 (2θ) range is shown in the inset. In the pattern of the $LaNiO_3$ sample treated

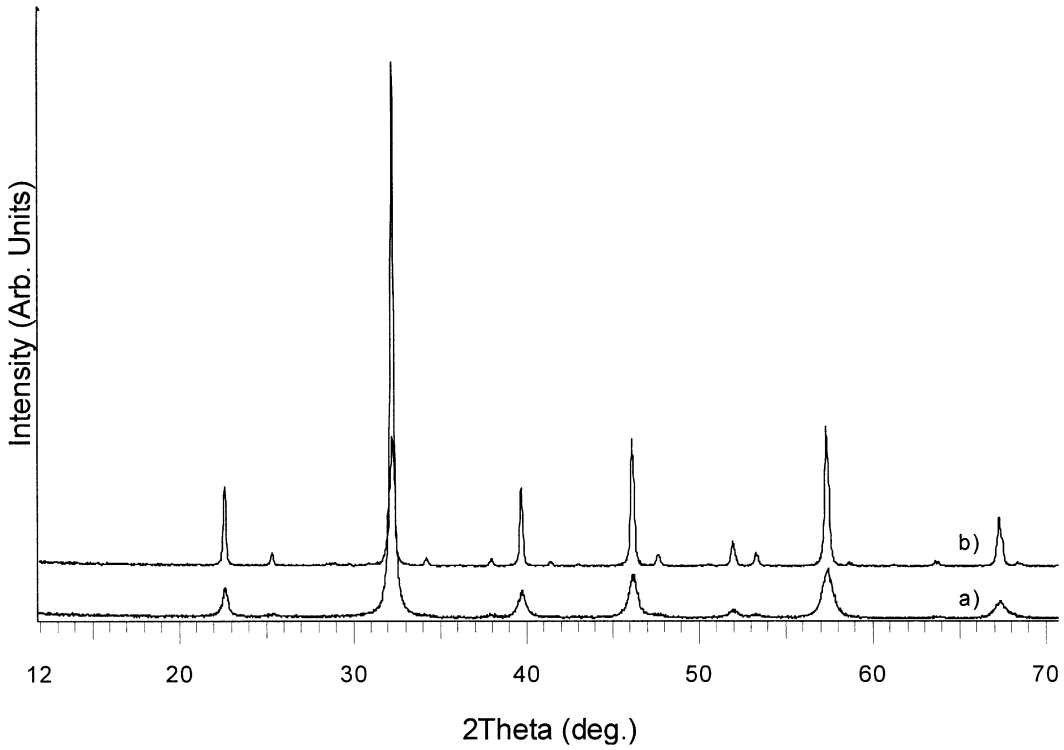

Fig. 1. XRD spectra of $LaFeO_3$ samples. XRD patterns have been collected after each calcination treatment, performed at 600, 700, 800, 900 and 1000 °C. Here only the spectra collected after the calcination treatments performed at 600 °C (a) and 1000 °C (b) are shown. All the reflections are attributed to the cubic and the orthorhombic phases respectively. Similar patterns are obtained for $LaNi_{0.3}Fe_{0.7}O_3$.

at 600 °C the peaks at 13, 23 and 29.5° (2θ) can be attributed to $La_2O_2CO_3$ (JC-PDF, card No. 481113) while the peaks at 37.5 and 43.5°(2θ) indicate the segregation of NiO (JC-PDF, card No.780643).

The peaks at 32.8, 47, and 58° (2θ) have been attributed to a cubic perovskite $LaNiO_3$ phase, (JC-PDF card No. 330710). From 700 to 900 °C in the diffraction patterns only the $LaNiO_3$ rhombohedral phase (JC-PDF, card No. 330711) has been detected. Thus, as reported in the literature,[15] the $LaNiO_3$ is stable in the rhombohedral phase. However, we found that after the treatment at 1000 °C the $LaNiO_3$ rhombohedral phase partially decomposed in NiO and $La_4Ni_3O_{10}$ (JC-PDF, card No. 831164). From these results we concluded that the $LaNiO_3$ is monophasic only in the range of 700–900 °C.

In Fig. 3 the difference in the shape and position of the reflection at about 32° (2θ) is shown for the tree samples heated at 600 and 1000 °C. Only for the $LaNiO_3$ the pattern at 900 °C is reported, since at 1000 °C different phases segregated. As a reference, the position of the reflections of the cubic (JC-PDF, card No. 750541) and orthorhombic (JC-PDF, card No. 742203) $LaFeO_3$, cubic (JC-PDF, card No. 330710) and rhombohedral (JC-PDF, card No. 330711) $LaNiO_3$ phases are shown.

In all the samples the temperature treatments have two evident effects on the XRD patterns: the first is the decreasing of the width, the second is the shift of the peak positions. In particular, the analysis of the XRD patterns revealed that, at a given temperature, the reflections shifted toward larger 2θ values increasing the Ni content, thus the unit cell volume increases with the Fe content. This has been ascribed to the larger ionic radius of Fe compared to that of Ni. The linear behavior of the lattice parameters as a function of sample stoichiometry, calculated in the approximation of pseudo-cubic structures by using the five most intense XRD reflections, is totally in accord with Provendier et al. results.[15]

Besides, for the samples with the same stoichiometry it is evident a peak shift, when the temperature of the treatment increases. In Fig. 4 the behavior of normalised volumes of the perovskite phases as a function of the thermal treatment is shown and compared with the literature results.[15,20,24] On the contrary of what expected the volume of cubic phases for all the samples decreased with the temperature of the treatment, probably because of the diffusion of defects and recrystallization processes that finally determine the phase transformation. When the stable phase is achieved (i.e. orthorhombic for the $LaFeO_3$ and $LaNi_{0.3}Fe_{0.7}O_3$ and rhombohedral for $LaNiO_3$) the normalised volumes are constant respect to the thermal treatments. All the volumes of the samples discussed in this paper are slightly larger than those reported in the literature. The origin of these differences may be the high density of defects introduced by the synthesis method.

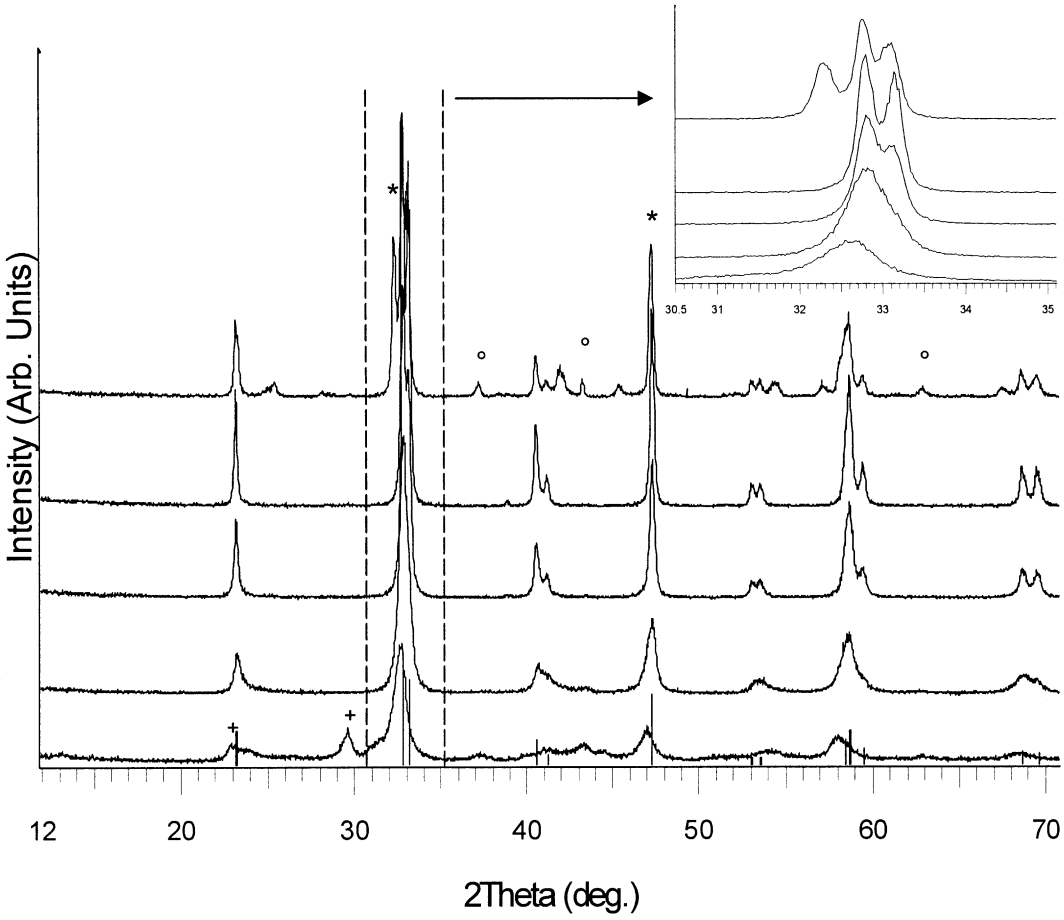

Fig. 2. XRD spectra of $LaNiO_3$ samples. XRD patterns have been collected after each calcination treatment, performed at (from the bottom) 600, 700, 800, 900 and 1000 °C. For clarity, in the inset the expansion of the 31–35 (2θ) range is shown. As a reference, the $LaNiO_3$ (JC-PDF, card No. 330711) pattern is also reported by means of vertical bars. At 600 °C the peaks at 13, 23 and 29.5° (2θ) can be attributed to $La_2O_2CO_3$ (JC-PDF, card No. 481113) (+). The peaks at 37.5 and 43.5° (2θ) indicate the segregation of NiO (JC-PDF, card No. 780643) (°). The peaks at 32.8, 47 and 58° (2θ) have been attributed to a $LaNiO_3$ cubic phase (JC-PDF, card No. 330710). At 1000 °C the peaks at 25.5, 32 and 42° (2θ) can be attributed to the $La_4Ni_3O_{10}$ (JC-PDF, card No. 831164) (*) phase.

The evolution with temperature of the average crystalline size of the $LaMO_3$ phases calculated by the Sherrer equation from the reflection width are shown in Fig. 5. These data indicate that the crystalline sizes increase monotonically with the calcination treatments. For each temperature treatment, the crystalline sizes of samples $LaFeO_3$ are the largest with exception of the sample treated at 800 °C. The great increment of the $LaNiO_3$ size at 800 °C may be related to the second order transformation from cubic to rhombohedral $LaNiO_3$ phase. Indeed, also for $LaFeO_3$ and $LaNi_{0.3}Fe_{0.7}O_3$ samples the largest increment in the crystalline size correspond to the second order phase transition from cubic to orthorhombic $LaFeO_3$, i.e. 900 °C. Moreover, the crystalline size of $LaNi_{0.3}Fe_{0.7}O_3$ samples are always smaller than that of $LaFeO_3$ samples. This confirms the fact that the presence of Ni inhibits the crystalline growth.[10]

Disorder effects due to oxygen non-stoichiometry have been studied by means of microraman spectroscopy, that is recognised to be sensitive to structural distortion in the local symmetry. Thus, this technique is expected to provide short range structural information.

Fig. 6 shows the microraman spectra of samples annealed at 700 °C, that, by means of XRD measurements, are found all monophasic with a cubic perovskite type of structure. The intensity and lineshape of the spectra below 200 cm^{-1} are not reported since the data are affected by the notch filter cutoff frequency. Even if the long-range symmetry of the three samples is the same, different spectra are obtained. Indeed for symmetry a cubic perovskite should not show any bands, as found in the spectrum collected for $LaNi_{0.3}Fe_{0.7}O_3$. As reported for $LaGaO_3$ doped materials,[25] the bands in the Raman spectra probably disappear because of disorder induced by the doping and the consequent nearly cubic symmetry of the structure. On the contrary, the bands detected in $LaFeO_3$ and $LaNiO_3$ point out that the local symmetry of these phases is lower than cubic and it is different from each other. The intense band at about 610 cm^{-1} can be attributed to the symmetry

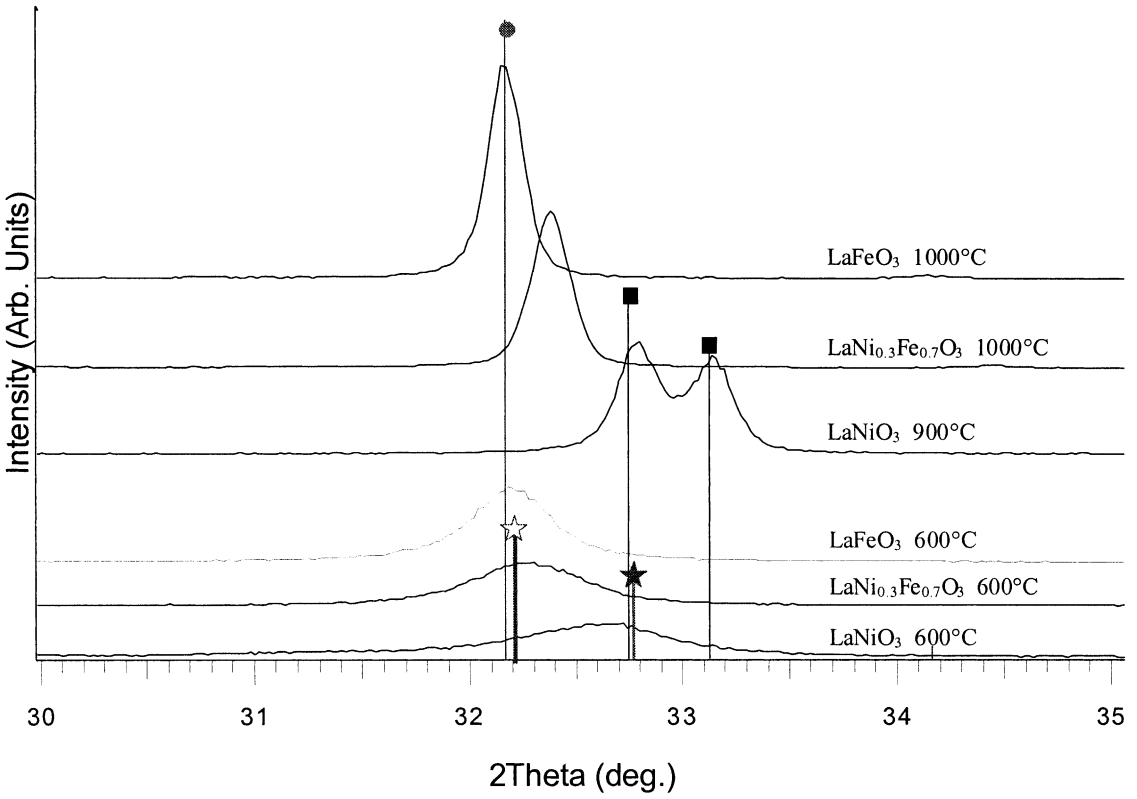

Fig. 3. XRD spectra of $LaMO_3$ samples, collected after the calcination treatment, performed at 600, and 1000 °C (except for the $LaNiO_3$ sample: the XRD reported pattern was collected after the annealing at 900 °C, because of some additional peak presence at 1000 °C, due to other segregated phases). As a reference, the position of the reflection of the cubic (JC-PDF, card No. 750541) and orthorhombic (JC-PDF, card No. 742203) $LaFeO_3$ and cubic (JC-PDF, card No. 330710) and rhombohedral (JC-PDF, card No. 330711) $LaNiO_3$ phase are reported by means of star, circle, filled star and square respectively.

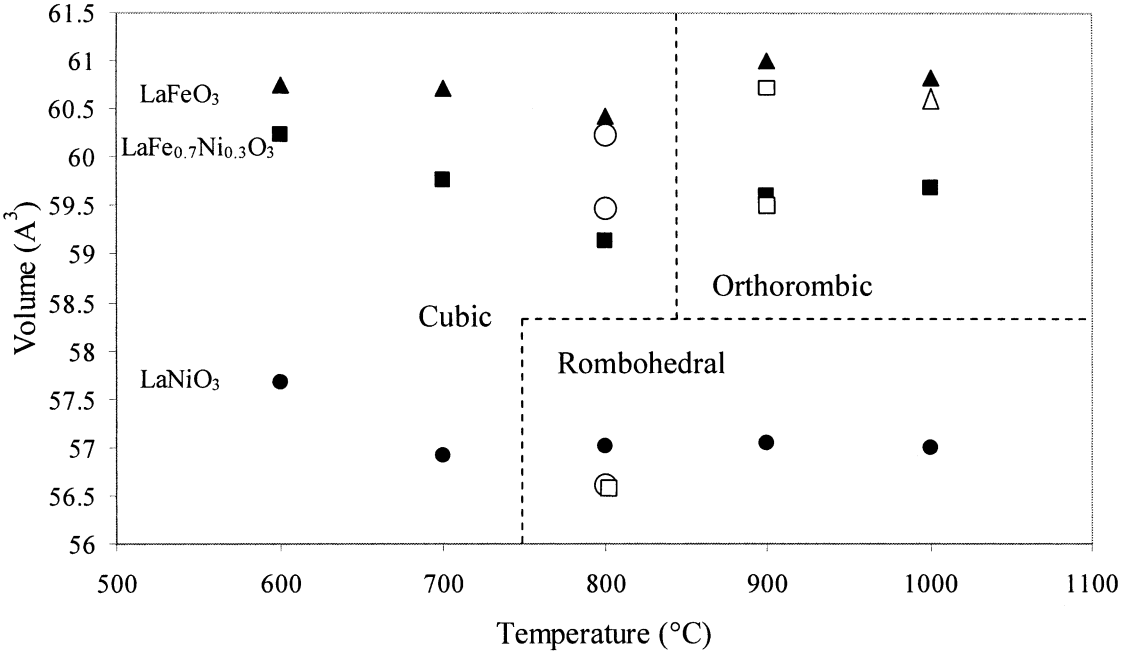

Fig. 4. The cell volumes, as a function of annealing temperature for all the samples (filled symbols). As a comparison Falcon et al. (□), Sangaletti et al. (△) and Provendier et al. results are also considered (○). See the text.

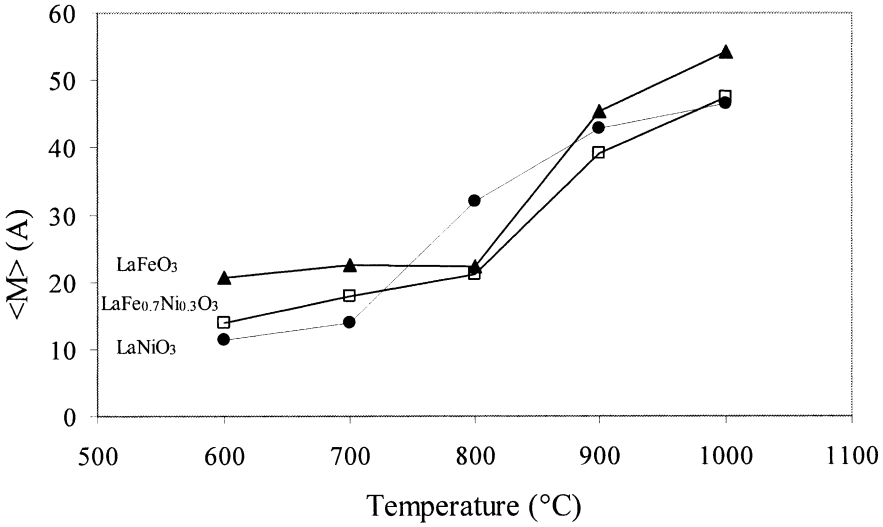

Fig. 5. Evolution with temperature of the average crystalline size $<M>$ of the $LaMO_3$ phases calculated by the Sherrer equation from the reflection width are shown. These data indicate that the crystalline sizes increase monotonically with the calcination treatments.

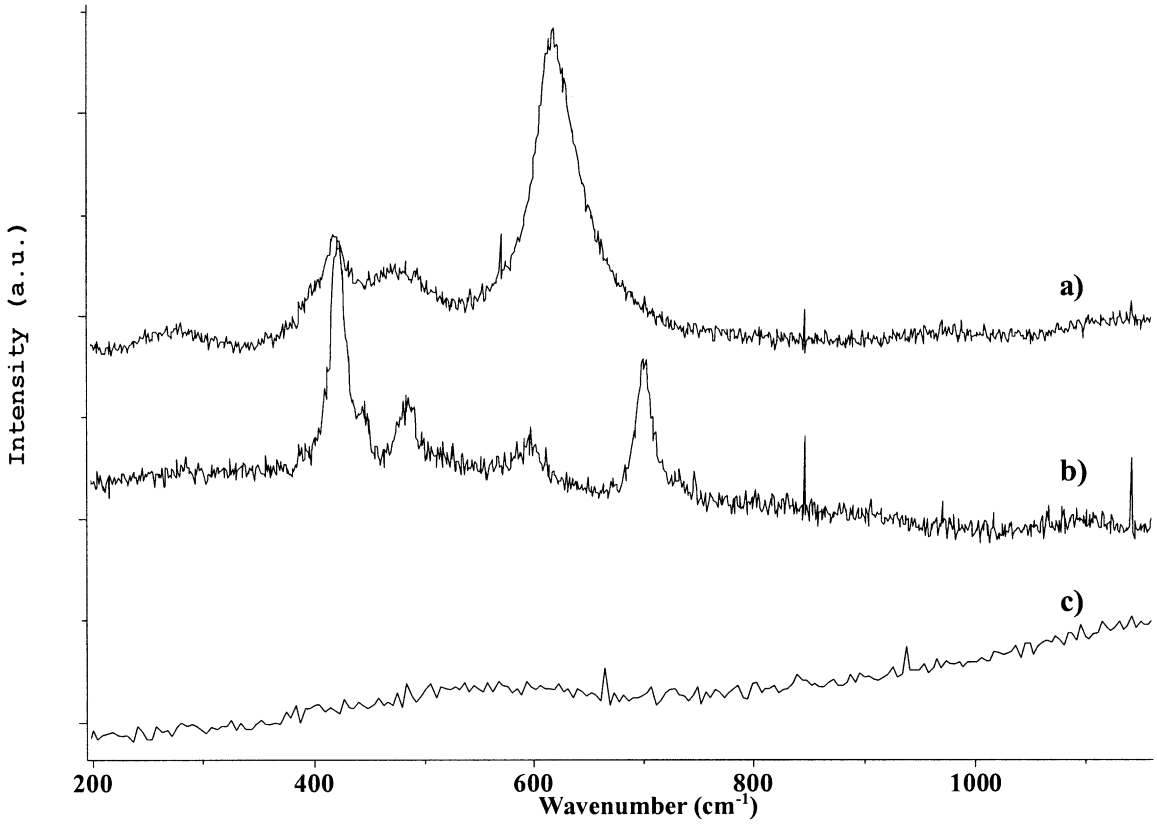

Fig. 6. Microraman spectra for all the samples annealed at 700 °C: (a) $LaFeO_3$, (b) $LaFeO_3$ and (c) $LaFe_{0.7}Ni_{0.3}O_3$.

stretching of the basal oxygen of the octahedra of the ion in the B site.[26]

In Fig. 6c the band at 690 cm^{-1} can be assigned to rhombohedral $LaNiO_3$ structure.[26] Thus, even if the long-range symmetry of the three samples is the same, locally different order has been detected. This result is very important when considering the functional properties of these materials that may be strongly influenced by distortions of the metal coordinations.

SEM analysis has been performed on samples $LaFeO_3$, $LaNiFeO_3$, and $LaNiO_3$ after thermal treatment at 600, 700, 800, 900 and 1000 °C and the morphological evolution of these materials are illustrated by the micrographs reported in Fig. 7.

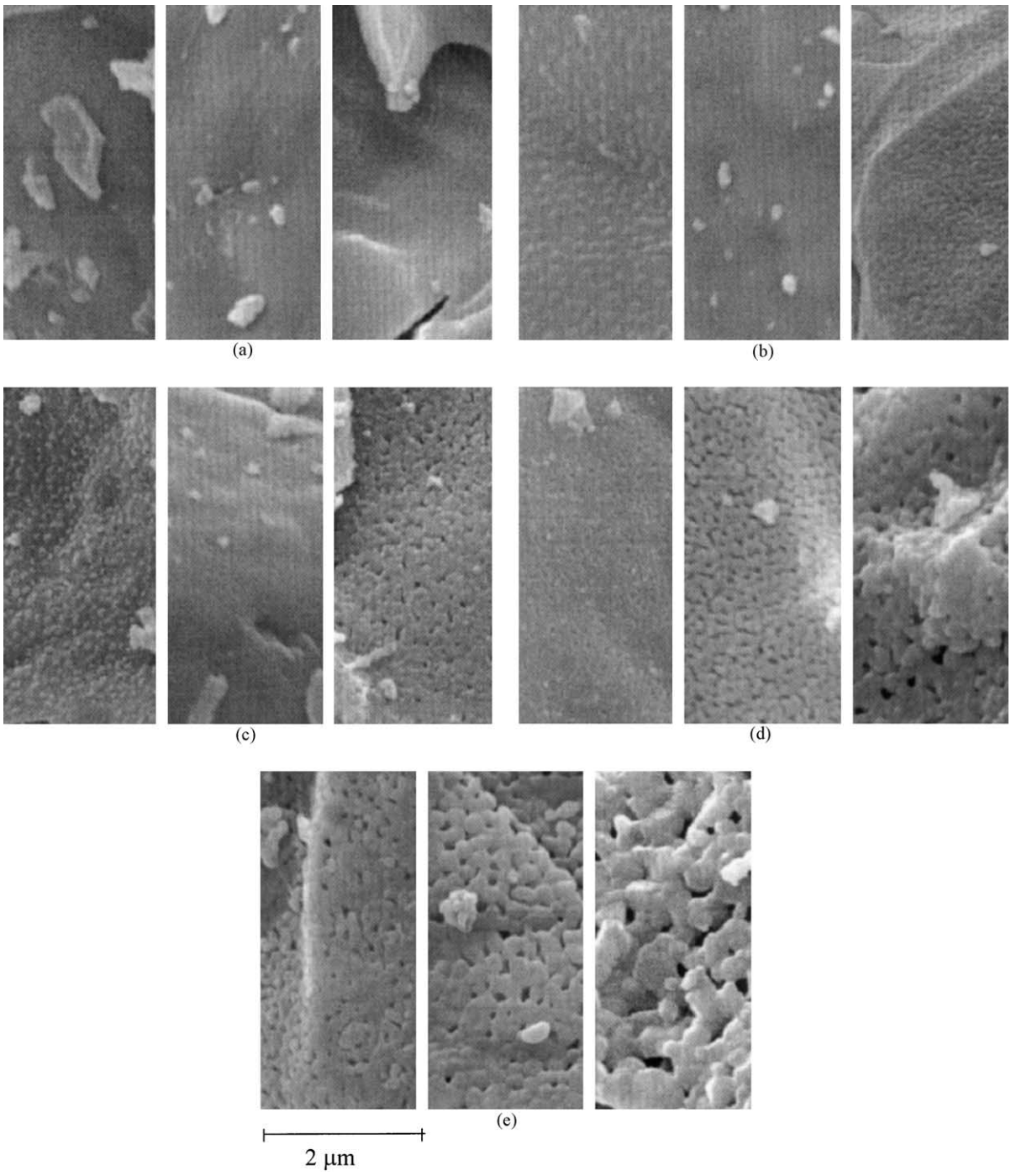

Fig. 7. SEM micrographs performed on $LaFeO_3$, $LaNi_{0.3}Fe_{0.7}O_3$ and $LaNiO_3$ samples respectively, after thermal treatment at 600 (a), 700 (b), 800 (c), 900 (d), and 1000 °C (e).

In all the samples the porosity increased with the temperature of the treatment. The porosity may be related to the phase transformation from cubic to the orthorhombic or to rhomboedral phases for $LaFeO_3$/$LaNi_{0.3}Fe_{0.7}O_3$ and $LaNiO_3$ respectively. The presence of the Ni in the structure seems to favor the granular morphology.

4. Conclusions

The samples were prepared by wet method without nitrate precursors. The main results of the characterization are the following:

- For low temperature treatment a cubic perovskite

phase is formed for $LaFeO_3$, $LaNi_{0.3}Fe_{0.7}O_3$ and $LaNiO_3$. The differences in the cell parameter may be related to the larger ionic radius of Fe compared to that of Ni.

- The recrystallization of the materials in the stable phase (orthorhombic for $LaFeO_3$/$LaNi_{0.3}Fe_{0.7}O_3$ and rhomboedral for $LaNiO_3$) is related to a large increment in the crystalline size.
- The microraman spectroscopy shows that, on the contrary of what found by XRD and reported in the literature, the short range symmetry of the phases of $LaFeO_3$, $LaNi_{0.3}Fe_{0.7}O_3$ and $LaNiO_3$ at 700 °C is orthorhombic, cubic and rhomboedral respectively. Thus these results show that the XRD study is not sufficient to structurally characterize these materials and the spectroscopy analysis may be important to understand their functional properties.
- SEM micrographs allow to follow the morphological changes due to the thermal treatment.

References

1. Peña, M. A. and Fierro, J. L. G., Chemical structures and performance of perovskite oxides. *Chem. Rev*., 2001, **101**, 1981–2017.
2. Kharton, V. V., Yaremchenko, A. A. and Naumovich, E. N., Research on the electrochemistry of oxygen ion conductors in the former Soviet Union. II. Perovskite-related oxides. *J. Solid State Electr*., 1999, **3**, 303–326.
3. Takemoto, M., Miyajima, T., Takayanagi, K., Ogawa, T., Ikawa, H. and Omata, T., Properties of transition metal oxides with layered perovskite structure. *Solid State Ionics*, 1998, **108**, 255 – 260.
4. Two, J. and Gallagher, P. K., In *Properties and Application of Perovskite Type Oxides*, ed. L. G. Tejuca and J. L. G. Fierro. Marcel Dekker, New York, 1993, p. 215.
5. Noriaki, H., Hideaki, S., Igor, S. and Kiyoyuki, T., Electronic band structure and lattice distortion in perovskite transition-metal oxides. *Physica B*, 1997, **237–238**, 11–13.
6. Wang, Z. W., The melting of Al-bearing perovskite at the core–mantle boundary. *Physics of the Earth and Planetary Interiors*, 1999, **115**, 219 –228.
7. Daturi, M., Busca, G. and Willey, R. J., Surface and structure characterization of some perovskite-type powders to be used as combustion catalysts. *Chem. Mater*., 1995, **7**, 2115–2126.
8. Zhong, Z. Y., Chen, K. D. and Ji, Y., Methane combustion over B-site partially substituted perovskite-type $LaFeO_3$ prepared by sol-gel method. *Applied Catalysis A: General*, 1997, **156**, 29–41.
9. Slagtern, A. and Olsbye, U., Partial oxidation of methane to synthesis gas-using La–M–O catalysts. *Applied Catalysis A*, 1994, **110**, 99–108.
10. Hayakawa, T., Harihara, H., Andersen, A. G., Suzuki, K., Yasuda, H., Tsunoda, T., Hamakawa, S., York, A. P. E., Yoon, Y. S., Shimizu, M. and Takehira, K., Sustainable $Ni/Ca_{1-x}Sr_xTiO_3$ catalyst prepared in situ for the partial oxidation of methane to synthesis gas. *Applied Catalysis A*, 1997, **149**, 391–410.
11. Provendier, H., Petit, C. and Kienneman, A., Steam reforming of methane on $LaNi_xFe_{1-x}O_3$ ($0 \leqslant x \leqslant 1$) perovskites. Reactivity and characterisation after test. *Comptes Rendus de l'Academie des Sciences Series IIC Chemistry*, 2001, **4**, 57–66.
12. Courty, P. H., Ajot, H., Marcilly, C. H. and Delmon, B., *Powder Technology*, 1973, **7**, 21.
13. Provendier, H., Petit, C., Roger, A. C. and Kienemann, A., Influence of the precursors on the formation of a trimetallic defined structure. Application on Ni catalysts used for syngas obtention. *Stud. Surf. Sci. Catal*., 1998, **118**, 285–294.
14. Provendier, H., Petit, C., Schmitt, J. L., Kienemann, A. and Chaumont, C., Characterisation of the solid solution La(Ni,Fe)O-3 prepared via a sol-gel related method using propionic acid. *Journal of Materials Science*, 1999, **34**, 4121–4127.
15. Provendier, H., Petit, C., Estournes, C., Libs, S. and Kienemann, A., Stabilisation of active nickel catalysts in partial oxidation of methane to synthesis gas by iron addition. *Applied Catalysis A*, 1999, **180**, 163–173.
16. Rapagnà, S., Provendier, H., Petit, C., Kienemann, A. and Foscolo, P. U., Development of catalysts suitable for hydrogen or syn-gas production from biomass gasification. *Biomass and Bioenergy*, 2002, **22**, 377–388.
17. JC-PDF database, International Centre for Diffraction Data, 1998.
18. EVA, copyright Bruker AXS Version 5.0, 1999.
19. Topas P, copyright Bruker AXS Version 1.0.1, 1999.
20. Falcon, H., Gaeta, A. E., Punte, G. and Carbonio, R. E., Crystal structure refinement and stability of $LaFe_xNi_{1-x}O_3$ solid solutions. *J. Solid State Chem*., 1997, **133**, 379–385.
21. Kharton, V. V., Vuskup, A. P., Naumovich, E. N. and Tikhonovich, V. N., Oxygen permeability of $LaFe_{1-x}Ni_xO_3$-delta solid solutions. *Materials Research Bulletin*, 1999, **34**, 1311–1317.
22. Depero, L. E. and Levrangi, P., Rigid-disordered models for inorganic structures—the case of zirconia nanopowders. *J. Solid State Chem*., 1994, **110**, 190–192.
23. Depero, L. E., Groppelli, S., Natali-Sora, I., Sangaletti, L., Sberveglieri, G. and Tondello, E., Structural studies of tungsten-titanium oxide thin films. *J. Solid State Chem*., 1996, **121**, 379–387.
24. Sangaletti, L., Depero, L. E., Allieri, B., Nunziante, P. and Traversa, E., An X-ray study of the trimetallic $La_xSm_{1-x}FeO_3$ orthoferrites. *Journal of the European Ceramic Society*, 2001, **21**, 719–726.
25. Inagaki, T., Miura, K., Yoshida, H., Fujita, J. and Nishimura, M., Raman studies of $LaGaO_3$ and doped $LaGaO_3$. *Solid State Ionics*, 1999, **118**, 265–269.
26. Martin-Carron, L., de Andres, A., Martinez-Lope, M. J., Casais, M. T. and Alonso, J. A., Raman phonons and light scattering in $RMnO_3$ (R = La, Pr, Nd, Ho, ErTb and Y) orthorhombic and hexagonal manganites. *Journal of Alloys and Compounds*, 2001, **323**, 494–497.